

Article

# Penttiptycene-Derived Fluorescence Turn-Off Polymer Chemosensor for Copper(II) Cation with High Selectivity and Sensitivity

Anting Chen <sup>1</sup>, Wei Wu <sup>1</sup>, Megan E. A. Fegley <sup>1</sup>, Sherrylene S. Pinnock <sup>1</sup>, Jetty L. Duffy-Matzner <sup>2</sup>, William E. Bernier <sup>1</sup> and Wayne E. Jones Jr. <sup>1,\*</sup>

<sup>1</sup> Department of Chemistry, Binghamton University, State University of New York, Binghamton, NY 13902, USA; achen47@binghamton.edu (A.C.); wwu39@binghamton.edu (W.W.); mfegley@binghamton.edu (M.E.A.F.); spinnoc1@binghamton.edu (S.S.P.); wbernier@binghamton.edu (W.E.B.)

<sup>2</sup> Department of Chemistry, Augustana University, Sioux Falls, SD 57197, USA; jetty.duffy@augie.edu

\* Correspondence: wjones@binghamton.edu; Tel.: +1-607-777-2421

Academic Editor: Po-Chih Yang

Received: 2 March 2017; Accepted: 21 March 2017; Published: 24 March 2017

**Abstract:** Fluorescent conjugated polymers (FCPs) have been explored for selective detection of metal cations with ultra-sensitivity in environmental and biological systems. Herein, a new FCP sensor, tmeda-PPpETE (poly[(penttiptycene ethynylene)-*alt*-(thienylene ethynylene)] with a *N,N,N'*-trimethylethylenediamino receptor), has been designed and synthesized via Sonogashira cross-coupling reaction with the goal of improving solid state polymer sensor development. The polymer was found to be emissive at  $\lambda_{\max}$  ~459 nm under UV radiation with a quantum yield of 0.119 at room temperature in THF solution. By incorporating diamino receptors and penttiptycene groups into the poly[(phenylene ethynylene)-(thiophene ethynylene)] (PPETE) backbone, the polymer showed an improved turn-off response towards copper(II) cation, with more than 99% quenching in fluorescence emission. It is capable of discriminating copper(II) cation from sixteen common cations, with a detection limit of 16.5 nM (1.04 ppb).

**Keywords:** fluorescence; conjugated polymers; penttiptycene; chemical sensor; copper sensor

## 1. Introduction

The development of chemical sensors has been a primary focus of environmental scientists for decades due to contamination of natural waters by toxic transition metal pollutants. Fluorescent conjugated polymers (FCPs) have received significant attention due to their ability to function as chemosensors in environmental and biological systems with both sensitivity and selectivity [1–5]. Based on rapid electron and energy transfer paths, these highly correlated one-dimensional systems have been found to demonstrate “million fold” sensitivity compared to monomolecular sensor analogues [6]. In most cases, the intrinsic electronic properties of the FCP backbones do not fulfill the selectivity requirements of most sensors. In response, various pendent groups known as “receptors” have been appended to the polymer side chains or at the end of the polymer chain [7]. Receptors such as crown ethers [8], amino group chelators [9], bi-pyridine and terpyridine ligands [10] and others have been evaluated based on their ability to bind metal cations selectively.

Copper is a naturally occurring trace element found in the earth’s crust and surface water. However, it can also enter water streams through industrial deposits, wood preservatives and plumbing systems. In the U.S., the Environmental Protection Agency (EPA) has a standard action level for copper of 1.3 ppm (~20  $\mu$ M) [11]. Copper is also one of the important trace elements

found in the living creatures. An adult human body contains about 80 mg of copper which mostly exist in various proteins and which function via redox processes [12,13]. However, excess copper may damage the cellular components and result in chronic disease, neurological disorder, and liver or kidney damage [14,15]. Copper has also been linked to Alzheimer's, Parkinson's and other neurodegenerative diseases [13,16]. Currently, the standard analytical method for testing copper in drinking water by the EPA is absorption spectrometry [17]. Other methods such as inductively coupled plasma mass spectroscopy (ICP-MS) [18] and electrochemical methods (cathodic or anodic stripping voltammetry) [19,20] are also used in other practice. Even though the accuracy of these instruments is high, and prized as "gold standards", they are quite expensive and often require sample preservation and preparation, as well as expert training. In addition, these methods cannot be used in biological and clinical practice, on-site tests and in situ studies. Thus, the need of developing a simple, rapid, and adaptable method is rising in sensor research. Fluorescent chemosensors have been extensively researched due to their fast and simple read-out, high selectivity and sensitivity, and overall low price.

Previously, the polymer tmeda-PPETE (Figure 1), *N,N,N'*-trimethylethylene-diamino receptors loaded on the thiophene ring of the poly[(phenylene ethynylene)-*alt*-(thiophene ethynylene)] (PPETE) backbone was studied [9,21,22]. This polymer has been shown to have a small fluorescence "turn-on" response when exposed to most metal cations in solution, but a significant quenching upon addition of  $\text{Cu}^{2+}$ . A more practical approach is to transfer the FCPs from solution to a solid-state matrix, and incorporate them into a field-based chemical sensing device [23–25]. Previous studies in the Jones group and others have shown that the photophysical properties of the solid state chemosensors are significantly affected by intermolecular interactions among polymer chains [26]. This phenomenon has been shown to significantly reduce the quantum efficiency of light emitting diodes (LEDs) and sensor devices. Thus, the transition from solution based sensor to a solid state suffers from the loss of sensitivity. In recent years, much effort has been put into chemical sensing improvements focused on minimizing the extent of polymer chain interaction to provide more efficient energy migration along the polymer chain [27,28].

In the attempt to decrease the effect of polymer self-quenching and  $\pi$ -stacking, a pentiptycene monomer was introduced into the polymer backbones. The rigid three-dimensional sterically hindered framework of the polymer backbones is known to prevent  $\pi$ -stacking of polymer chains [29]. When combined with other groups, pentiptycene can also be part of the analyte capture and recognition unit for cations and anions in small molecule sensors [30,31]. In the interest of developing cation recognition FCPs containing the pentiptycene unit, the synthesis of tmeda-PPpETE (poly[(pentiptycene ethynylene)-*alt*-(thienylene ethynylene)] with a *N,N,N'*-trimethylethylenediamino receptor) and its model polymer butyl-PPpETE are presented, together with detailed photophysical studies and sensing abilities of this new material (Figure 1).

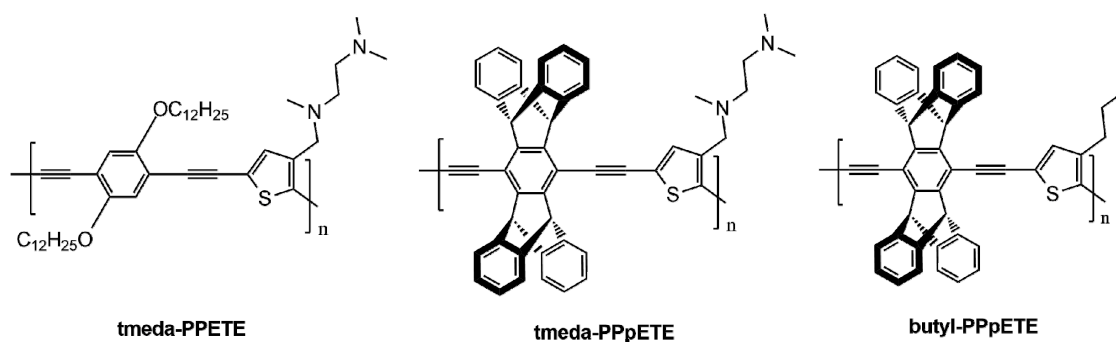


**Figure 1.** Structures of tmeda-PPETE, tmeda-PPpETE and butyl-PPpETE.

## 2. Materials and Methods

### 2.1. Materials

Tetrakis(triphenylphosphine)palladium ((PPh<sub>3</sub>)<sub>4</sub>Pd), copper(I) iodide (CuI), tetrahydrofuran (THF), diisopropylamine (*i*-Pr<sub>2</sub>NH), 2,5-dibromo-3-butylthiophene and all other chemicals were purchased from Sigma-Aldrich (St. Louis, MO, USA), Fisher Scientific (Pittsburgh, PA, USA), Alfa Aesar (Ward Hill, MA, USA) or Acros Organics (Morris Plains, NJ, USA) and used as received unless otherwise noted. For air-sensitive synthetic steps, solvents were freshly distilled and stored under a nitrogen atmosphere prior to use.

### 2.2. General Methods

NMR spectra were obtained at room temperature on a Bruker Avance III 600 spectrometer (Billerica, MA, USA). IR spectra were obtained on an FT-IR Bruker Equinox55 spectrometer at a resolution of 2 cm<sup>-1</sup> with potassium bromide (KBr) pellets. The molecular weights and polydispersity distribution were determined by gel permeation chromatography (GPC) and performed by Corning Incorporated in Corning, NY, USA using THF as the mobile phase at 40 °C with a flow rate of 1.0 mL/min. The columns are calibrated using polystyrene standards ranging from 160–6,980,000 using EasiCal PS-1&2 kits. UV-Visible spectra were obtained on a Shimadzu UV-2600 UV-Visible spectrometer (Kyoto, Japan) in THF solution using 1 cm quartz cuvette cells. Fluorescence spectra were measured on a Shimadzu RF-6000 Spectro fluorophotometer. The instrument uses a 150 W Xenon arc lamp and a monochromator with 1300 grooves per mm concave blazed holographic gratings (F/2.5). The chemosensor solutions were prepared by dissolving a specific amount of chemosensor in THF to prepare a 250 μM stock solution (with respect to the polymer repeat unit), followed by a dilution to 5 μM. All metal cation solutions were prepared by dissolving their metal chlorides in water, in order to prepare a 0.01 M stock solution, followed by a dilution into 250 μM. Metal sensing tests were conducted by titration of 250 μM metal chloride solutions via micropipette into 3 mL of the 5 μM chemosensor polymer solution in a 1 cm quartz cuvette cell followed by thorough mixing. In the selectivity test, the mole ratio of the polymer repeating unit and the metal cation were fixed at 1:1 ratio. In the titration experiment, the concentration of the polymer was fixed at 5 μM while various amount of metal cation solution were added. It was assumed that using a concentrated stock solution could minimize the influence of water on the fluorescence of the polymer. All solutions were used within 24 h from preparation. All emission experiments were repeated at least three times, and the data was very reproducible with negligible variance. The fluorescence quantum yields of all polymers were determined relative to the standard, quinine sulfate, in 0.5 M sulfuric acid (H<sub>2</sub>SO<sub>4</sub>) solution with a quantum yield of 0.546 when excited at 365 nm [32].

### 2.3. Synthesis

The monomers, *N*-(2,5-dibromothiophene-3-ylmethyl)-*N,N,N'*-trimethylethan-1,2-diamine and 6,13-diethynyl-5,7,12,14-tetrahydro-5,14:7,12-bis([1,2-benzo) pentacene, were prepared by modifying previous literature methods (Scheme 1) [9,33–35]. The polymers, tmeda-PPpETE and butyl-PPpETE were prepared by a step growth polymerization via Sonogashira reaction: a palladium catalyzed cross-coupling of aromatic halides on the thiophene ring and the terminal alkynes on the center ring of the pentiptycene group. Synthesis of butyl-PPpETE can be found in the supplementary materials.

*6,13-diethynyl-5,7,12,14-tetrahydro-5,14:7,12-bis([1,2]benzo)pentacene* (**pentiptycene monomer, M1**) (white powder, yield 86.19%) <sup>1</sup>H-NMR (600 MHz, CDCl<sub>3</sub>, δ<sub>ppm</sub>): 7.35 (q, 4H), 6.95 (q, 4H), 5.82 (s, 2H), 3.68 (s, 2H). FT-IR (ν<sub>max</sub> cm<sup>-1</sup>, KBr): 3301, 3065, 3019, 2977, 2858, 1457, 1381, 1304, 1256, 1218, 1190, 1174, 1150, 1065, 748, 678, 661, 615, 602, 565, 449.

*N*-(2,5-dibromothiophene-3-ylmethyl)-*N,N,N'*-trimethylethan-1,2-diamine (**tmeda-thiophene monomer, M2**) (light yellow oil, yield 67.87%) <sup>1</sup>H-NMR (600 MHz, CDCl<sub>3</sub>, δ<sub>ppm</sub>): 6.97 (s, 1H), 3.42 (s, 2H), 2.45 (q,

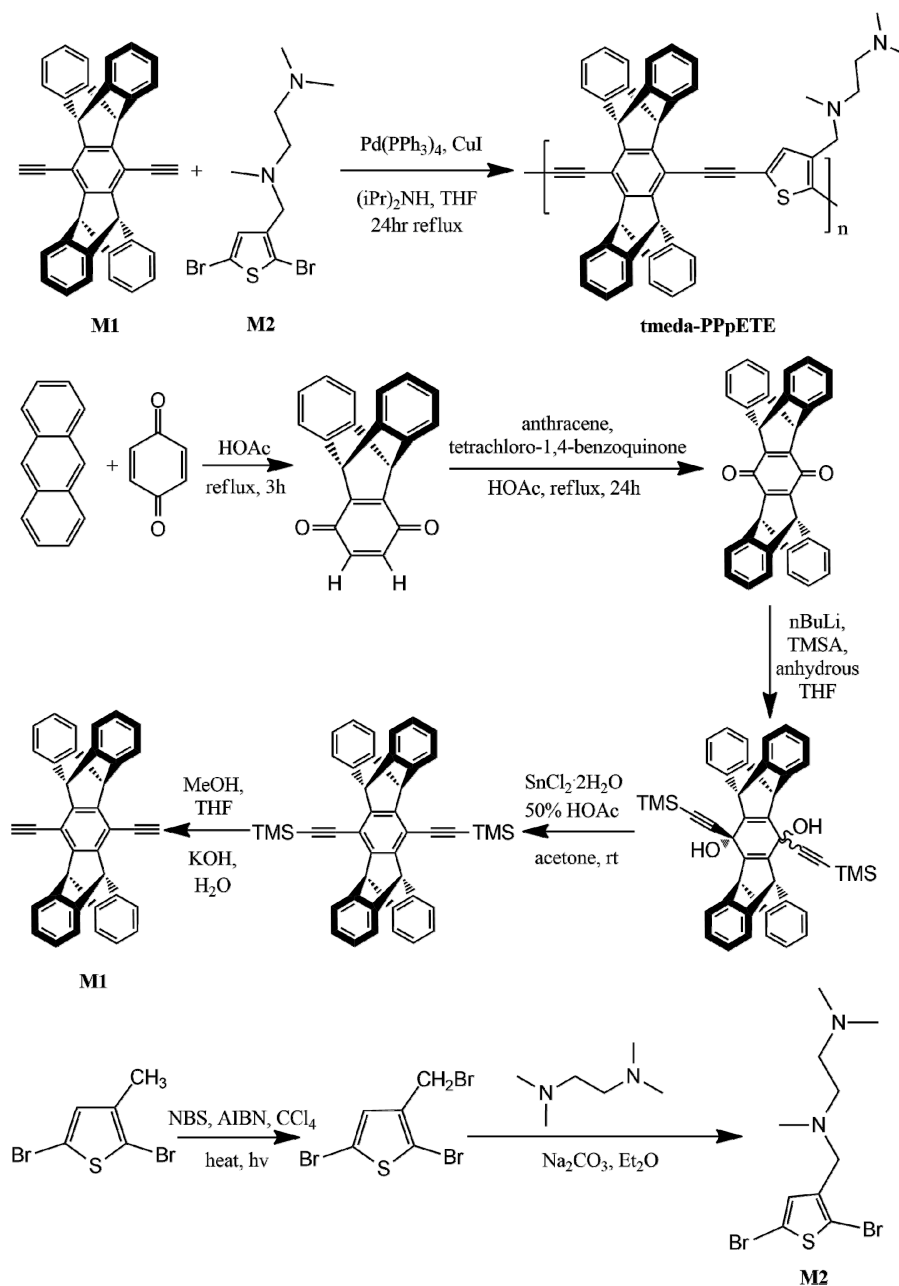
4H), 2.23 (d, 6H). FT-IR ( $\nu_{\max}$   $\text{cm}^{-1}$ , KBr): 3097, 2973, 2940, 2853, 2814, 2766, 2716, 1544, 1457, 1424, 1343, 1284, 1267, 1168, 1125, 1077, 1036, 1005, 981, 961, 912, 874, 836, 787, 700, 661, 580, 474.

Poly[2,5-(3-[*N*-methyl-*N*-(*N*',*N*'-dimethyl-2-ethanamino)methylamino] thiophenediyl)-1,2-ethynediyl-6,13-(5,7,12,14-tetrahydro-5,14,7,12-di[1,2]benzeno-pentacenediyl)-1,2-ethynediyl] (**tmeda-PPpETE**). *i*-Pr<sub>2</sub>NH (5 mL) was added to a mixture of *N*-(2,5-dibromothiophene-3-ylmethyl)-*N,N,N'*-trimethylethan-1,2-diamine (0.374 g, 1.05 mmol), 6,13-diethynyl-5,7,12,14-tetrahydro-5,14:7,12-bis([1,2]-benzeno)-pentacene (0.479 g, 1.0 mmol), Pd(PPh<sub>3</sub>)<sub>4</sub> (58 mg, 0.05 mmol) and CuI (20 mg, 0.10 mmol) in 30 mL anhydrous THF under nitrogen atmosphere. The resulting mixture was stirred for 5 h for the monomers to dissolve and then refluxed for 24 h. The reaction mixture was cooled down to room temperature and the residual solid in the reaction mixture was filtered out. The filtrate was concentrated under vacuum. Chloroform (30 mL  $\times$  2) was added to extract the product and the organic phase was washed with water (50 mL  $\times$  2) and dilute NaHCO<sub>3</sub> solution (5 wt %, 50 mL  $\times$  2). The organic phase was dried over MgSO<sub>4</sub>, and the solvent was removed under reduced pressure. The residue was washed with hot water, hot methanol and hot acetone, sequentially. The crude product was dissolved in minimum amount of chloroform and precipitated in methanol. The precipitation product was filtered and dried to give a bright yellow solid (0.545 g, yield 81%). GPC (in THF, with polystyrene standard)  $\overline{M}_w = 3.33 \times 10^4$  g/mol; polydispersity index (PDI) = 2.11. <sup>1</sup>H-NMR (600MHz, CDCl<sub>3</sub>,  $\delta_{\text{ppm}}$ ): 7.76 (1H), 7.53 (8H), 7.07 (8H), 6.00–5.96 (4H), 4.13 (2H), 2.91–2.66 (4H), 2.39–2.34 (9H). UV-Vis  $\lambda_{\max} = 416$  nm. Emission  $\lambda_{\max} = 459$  nm. FT-IR ( $\nu_{\max}$   $\text{cm}^{-1}$ , KBr): 3065, 3022, 2967, 2934, 2853, 2814, 2766, 2182, 1455, 1379, 1310, 1256, 1179, 1153, 1022, 928, 853, 750, 671, 566. The formation of an internal ethynyl link was confirmed by the presence of the 2182  $\text{cm}^{-1}$  stretch.

### 3. Results and Discussion

#### 3.1. Synthesis and Characterization

The polymerization of **tmeda-PPpETE** was carried out employing the Sonogashira cross-coupling of the aromatic halides of the receptor loaded thiophene monomer (**M2**), and the terminal alkynes on the center ring of the pentiptycene monomer (**M1**) (Scheme 1) [36]. To further study the impact of the diamino receptor, a model polymer, butyl-PPpETE was also designed and synthesized, where the diamino receptor was substituted by a butyl group [9]. **M1** and **M2** were synthesized according to literature descriptions with small adjustments (Scheme 1). All of the monomers and the polymers were well characterized by <sup>1</sup>H-NMR and FT-IR (details in the Experimental Section). The NMR spectra of **tmeda-PPpETE** and the corresponding monomers were shown in Figure 2a. All the peaks that correspond to the protons in **tmeda-PPpETE** have been clearly assigned. The success of polymerization was noted by the disappearance of the terminal alkyne peak at 3.68 ppm in the polymer NMR. It is also worth mentioning that the peak assigned to the aromatic proton on the thiophene (peak A in Figure 2a) shifted from 6.97 ppm to 7.76 ppm, and the methylene protons' peak (peak B in Figure 2a) also shifted from 3.42 ppm to 4.13 ppm. These huge shifts can be assigned to the deshielding effect from the triple bonds [37], which also indicate the formation of internal ethynyl link. Extra evidence of polymerization is also found in the FT-IR (Figure 2b). In the pentiptycene monomer spectra, the acetylenic C-H stretching vibration has a sharp absorption at 3301  $\text{cm}^{-1}$ . This peak disappeared in the **tmeda-PPpETE** polymer spectra; instead, a broad, weak absorption around 2182  $\text{cm}^{-1}$  appeared, consistent with the formation of an internal ethynyl link.



**Scheme 1.** Synthesis of tmeda-PPpETE and its corresponding monomers.

The poly [*p*-(phenyleneethynylene)-*alt*-(thiyleneethynylene)] backbone was selected because of its intense fluorescence in the visible region of the electromagnetic spectrum [10]. The tmeda diamino receptor has previously been shown to quench the PPE fluorescence by a Dexter type mechanism [22]. The pentiptycene group has a rigid three-dimensional structure, which has been widely used in conjugated polymers to prevent inter-molecular chain quenching in higher concentrations as well as in the solid state [29,38]. It is also widely accepted that this group can recognize nitrate explosives in very low concentrations in aqueous solution as well as in air [39,40]. Some computational studies suggested that this electron-rich group has two types of cavities: a large cavity near the central ring consisting of the three benzene rings, and a small cavity on the side consisting of two benzene rings. Small molecule analytes (such as nitrate explosives) are more likely to fall into the small cavity because the large cavity suffers from steric crowding [41]. In some small molecule sensors, the pentiptycene group was found to participate in recognition of cations or anions [30,31]. The newly designed FCP, tmeda-PPpETE,

containing both the diamino receptor and the pentiptycene group, showed an interesting change in sensing copper(II) ions.

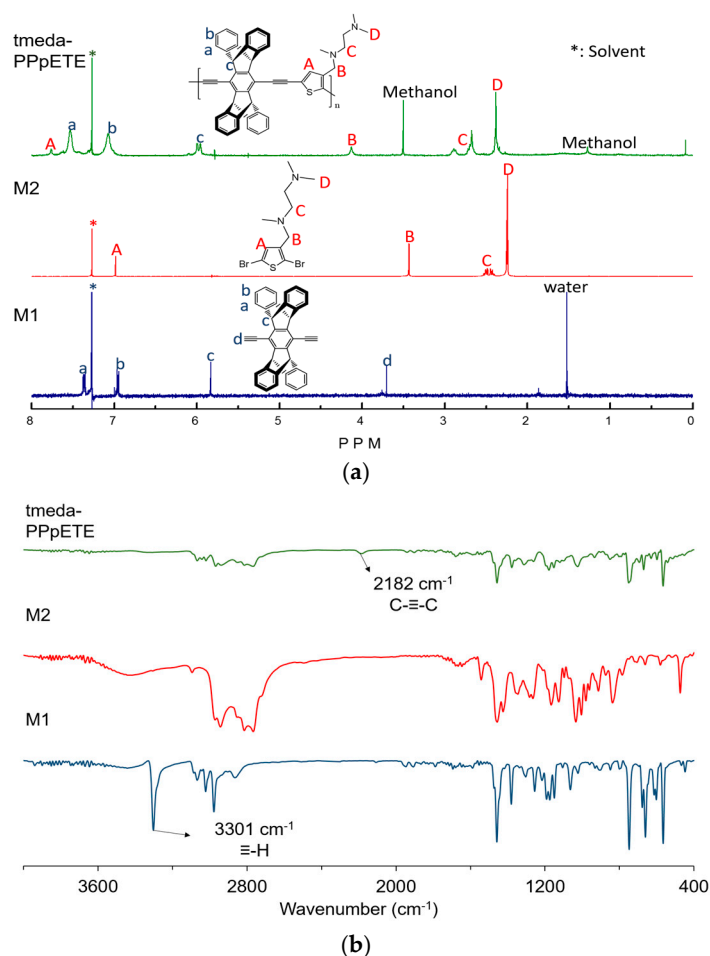


**Figure 2.** (a) <sup>1</sup>H-NMR (600 MHz, CDCl<sub>3</sub>) and (b) FT-IR of the tmeda-PPpETE polymer and the corresponding monomers.

The polymers tmeda-PPpETE and butyl-PPpETE are soluble in common organic solvents, such as chloroform and THF. This enables processability for application and fabrication of chemosensor systems. The molecular weight of these polymers was determined by GPC analysis with polystyrene as the standard. The molecular weight and polydispersity index were summarized in Table 1. tmeda-PPpETE has a weight average molecular weight ( $\overline{M}_w$ ) of  $3.33 \times 10^4$  g/mol (polydispersity index (PDI) = 2.11), which corresponds to a weight average degree of polymerization  $X_w \approx 49.5$  (~99 -Ph-C≡C-units). butyl-PPpETE has a slightly lower molecular weight, ( $\overline{M}_w$ ) of  $1.16 \times 10^4$  g/mol (PDI = 2.63), which corresponds to a  $X_w \approx 18.9$ . The moderate conjugation and chain length was expected to provide an excellent processability of the polymer material, and, at the same time, sustain a superb “molecular wire” effect yielding signal amplification [1,8].

**Table 1.** Summary of molecular weight and photophysical properties of polymers.

| Polymer Name | $\overline{M}_w$ (g/mol) | $\overline{M}_n$ (g/mol) | PDI  | Absorption $\lambda_{max}$ (nm) | Emission $\lambda_{max}$ (nm) | Fluorescence Quantum Yield |
|--------------|--------------------------|--------------------------|------|---------------------------------|-------------------------------|----------------------------|
| tmeda-PPpETE | $3.33 \times 10^4$       | $1.58 \times 10^4$       | 2.11 | 416                             | 459                           | 0.119                      |
| butyl-PPpETE | $1.16 \times 10^4$       | $4.43 \times 10^3$       | 2.63 | 418                             | 463                           | 0.402                      |

### 3.2. Photophysical Properties

The normalized UV-Visible absorption and photoluminescence emission spectra of tmeda-PPpETE and the model butyl-PPpETE are shown in Figure 3 and the photophysical data are summarized in Table 1. The polymer concentration for all photophysical experiments was maintained at 5  $\mu\text{M}$  with respect to the polymer repeating unit. The polymer, tmeda-PPpETE, has an absorption from 300 nm to 480 nm and the emission maximum is around 460 nm. The polymer solutions have a light-yellow color and a strong blue emission under UV irradiation. The absorption peak can be assigned to the  $\pi\text{-}\pi^*$  transition from the conjugated polymer backbone [42]. Compared to other polymers containing poly[(phenylene ethynylene)-(thiophene ethynylene)] (PPETE) backbone [9,10], the absorption peaks are blue shifted. The addition of the rigid pentiptycene group increased the  $\pi\text{-}\pi^*$  transition energy, and decreased the intermolecular interaction and “self-quenching”. The photoluminescence emission of the sensor and model polymers contained a narrow peak maximum and a shoulder, which can be assigned to a single transition with vibronic structure [10]. Compared to the model polymer, butyl-PPpETE, the absorption and emission maxima of tmeda-PPpETE are both slightly blue shifted. This was also observed in previous reports on tmeda-PPETE and its model polymer [9]. The similarity in absorption and emission spectra between butyl-PPpETE and tmeda-PPpETE indicated the introduction of the diamino receptor does not lead to a significant electronic or structural distortion of the polymer backbones. The fluorescent quantum yield of tmeda-PPpETE was found to be 0.119, which is similar to other PPETE systems [9,43]. This is also sufficient to be used as a sensory material. Compared to butyl-PPpETE, which has a fluorescent quantum yield of 0.402, tmeda-PPpETE has a much lower quantum yield. The introduction of the diamino receptor results in a photo-induced electron transfer (PET) to the excited state on the polymer backbone and the resulting loss of fluorescence [9].

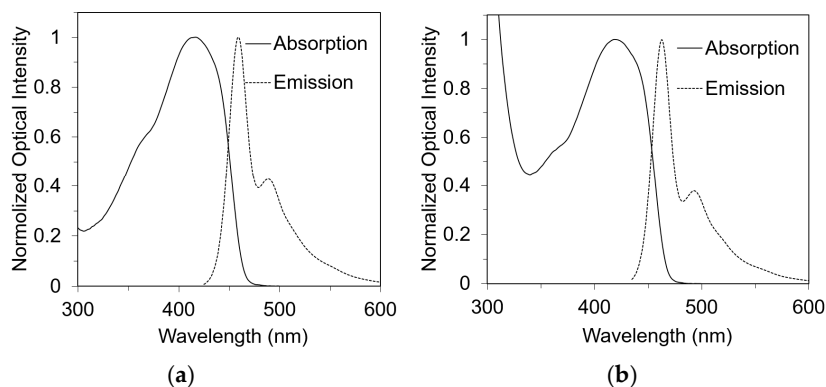


**Figure 3.** UV-Visible and emission spectra of (a) tmeda-PPpETE and (b) butyl-PPpETE in THF solution at room temperature.

### 3.3. Cation Selectivity

Fourteen representative metal ions ( $\text{Li}^+$ ,  $\text{Na}^+$ ,  $\text{K}^+$ ,  $\text{Mg}^{2+}$ ,  $\text{Ca}^{2+}$ ,  $\text{Mn}^{2+}$ ,  $\text{Fe}^{2+}$ ,  $\text{Fe}^{3+}$ ,  $\text{Co}^{2+}$ ,  $\text{Ni}^{2+}$ ,  $\text{Cu}^{2+}$ ,  $\text{Zn}^{2+}$ ,  $\text{Cd}^{2+}$ ,  $\text{Hg}^{2+}$ ) as well as  $\text{H}^+$  and  $\text{NH}_4^+$  cations were selected as representative analytes in this study. The cation titrations were carried out under the same conditions as previous studies with both the concentration of the polymer and the analyte held at 5  $\mu\text{M}$  [44,45]. The average values of the fluorescent intensity ( $I$ ) and the intensity change at the emission maximum upon titrating cation solutions were shown in Figure 4 (for fluorescent enhancement, the intensity change was expressed as  $I/I_0$ ; for fluorescent quenching, the intensity change was expressed as  $-I_0/I$ , where the negative sign means the decrease in fluorescent intensity). As an electron-rich group, the pentiptycene tends to be attracted to electron withdrawing groups [29,40,41]. However, its interactions with metal cations are less well known in the literature. Yang et al. [30] presented a pentiptycene-bispyrenyl system, which was selective towards  $\text{Ca}^{2+}$  and  $\text{Cd}^{2+}$ . In addition, a blue shift was observed in response to  $\text{Cu}^{2+}$ , where

the cation interacted with the system through a cation- $\pi$  interaction. To study the mechanism of the metal cation binding, whether it is solely dependent on the diamino group or the pentaptycene group, played a role in the binding, metal cation screening was also performed on the model butyl-PPpETE polymer in the same manor.

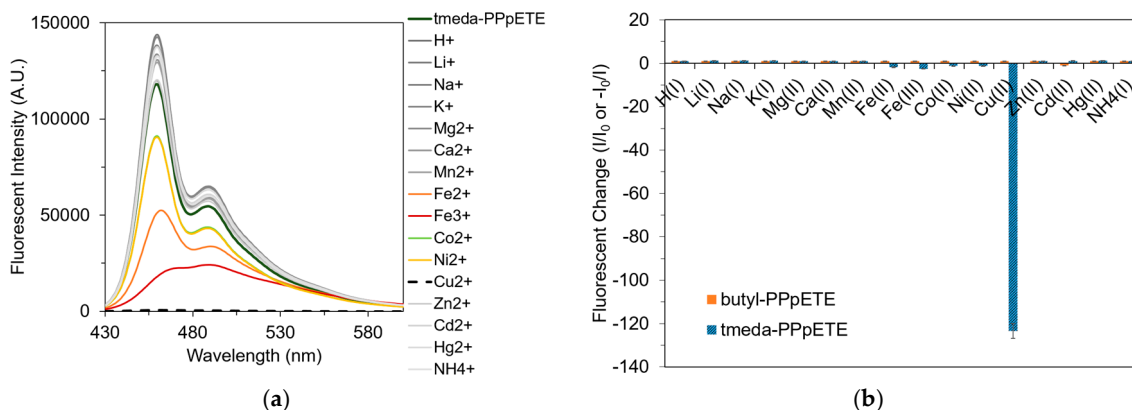


**Figure 4.** (a) emission spectra of tmeda-PPpETE and (b) the corresponding fluorescence response of tmeda-PPpETE and butyl-PPpETE to various 5  $\mu$ M cations in room temperature solution. Concentration of polymers (with respect to repeat unit) were fixed at 5  $\mu$ M.

For most cations, no significant change in fluorescence was observed; most of them showed a slight fluorescent turn-on response for both tmeda-PPpETE and the model butyl-PPpETE. However, addition of  $\text{Cu}^{2+}$  to tmeda-PPpETE caused significant fluorescent quenching, resulting more than 99% quenching at  $\lambda_{\text{max}} = 459$  nm (Figure 4). The intensity of fluorescence at the  $\lambda_{\text{max}}$  is two magnitudes (more than 120-fold) lower compared to the initial fluorescence. The “turn-off” response of tmeda-PPpETE towards  $\text{Cu}^{2+}$  is improved from tmeda-PPETE [22]. In the case of tmeda-PPETE, only 98% of the fluorescence was quenched at saturation. The mechanism of the fluorescence quenching by  $\text{Cu}^{2+}$  was similar to tmeda-PPETE, and the enhanced performance was the result of the addition of the pentaptycene group, which prevented  $\pi$ -stacking and increased the quantum yield of the polymer. Titration of  $\text{Fe}^{2+}$ ,  $\text{Fe}^{3+}$ ,  $\text{Co}^{2+}$  and  $\text{Ni}^{2+}$  also decreased the fluorescence but much less significantly. It was also noticed that addition of  $\text{Cd}^{2+}$  resulted in a slight decrease of fluorescence of the model butyl-PPpETE polymer, but the same response was not observed in tmeda-PPpETE.

As shown in Figure 5, an interference study was carried out. Cuvette (a) contains the tmeda-PPpETE solution in THF, which showed an intense blue fluorescence under UV light. Cuvette (b) was the polymer solution upon addition of  $\text{Cu}^{2+}$ , and the fluorescent quenching effect was visible to the naked eye. In Cuvette (c), 15 selected cations were added to the polymer solution, and the result was a slight decrease in fluorescent intensity, which was consistent with the fluorescent emission spectra. This was because  $\text{Fe}^{2+}$ ,  $\text{Fe}^{3+}$ ,  $\text{Co}^{2+}$  and  $\text{Ni}^{2+}$  can also partially quench the fluorescence, however not significantly. Cuvette (d) contained all the cations including  $\text{Cu}^{2+}$ , which quenched the fluorescence significantly, demonstrating that tmeda-PPpETE can be a viable  $\text{Cu}^{2+}$  sensor. Comparing cuvette (b) and (d), it was noted that a small portion of fluorescent present when there was interference from other cations. In the previous study [46], the polymer tmeda-PPETE was preloaded with  $\text{Cu}^{2+}$ , which quenches the initial fluorescence, and then a metal-polymer hybrid system can work as a turn-on sensor for iron cations. It is possible that, in the case of tmeda-PPpETE, a similar process was present where a tmeda-PPpETE/ $\text{Cu}^{2+}$  complex may be a turn-on sensor for other cations. Further studies are needed to explore the multi-ion interaction with tmeda-PPpETE.



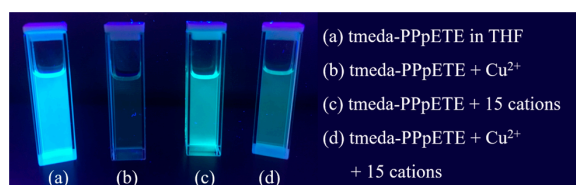


**Figure 5.** Interference studies on the tmeda-PPpETE polymer sensor: (a) 5  $\mu\text{M}$  tmeda-PPpETE in THF; (b) 5  $\mu\text{M}$  tmeda-PPpETE in THF after the addition of  $\text{Cu}^{2+}$  (5  $\mu\text{M}$ ); (c) 5  $\mu\text{M}$  tmeda-PPpETE in THF after the addition of  $\text{Li}^+$ ,  $\text{Na}^+$ ,  $\text{K}^+$ ,  $\text{Mg}^{2+}$ ,  $\text{Ca}^{2+}$ ,  $\text{Mn}^{2+}$ ,  $\text{Fe}^{2+}$ ,  $\text{Fe}^{3+}$ ,  $\text{Co}^{2+}$ ,  $\text{Ni}^{2+}$ ,  $\text{Zn}^{2+}$ ,  $\text{Cd}^{2+}$ ,  $\text{Hg}^{2+}$ ,  $\text{H}^+$  and  $\text{NH}_4^+$  (5  $\mu\text{M}$  each); (d) same as (c) except  $\text{Cu}^{2+}$  (5  $\mu\text{M}$ ) was also added. The image was taken under a commercial UV lamp (excitation wavelength: 365 nm).

### 3.4. Sensitivity

To evaluate the efficiency of tmeda-PPpETE as a  $\text{Cu}^{2+}$  sensor probe, the fluorescent emission spectra were monitored in response to a titration with various amounts of  $\text{Cu}^{2+}$  in aqueous solutions of tmeda-PPpETE (Figure 6 and Figure S4). To study the interference from other metal cations, fluorescent response of tmeda-PPpETE upon addition of  $\text{Fe}^{2+}$ ,  $\text{Fe}^{3+}$ ,  $\text{Co}^{2+}$  and  $\text{Ni}^{2+}$  was also studied (Figure 6). The fluorescence changes of tmeda-PPpETE upon adding  $\text{Cu}^{2+}$  was very dramatic and reached saturation at a very low concentration. About 80% of fluorescence was quenched at the  $\text{Cu}^{2+}$  concentration of 1.5  $\mu\text{M}$ ; at the concentration of 4.1  $\mu\text{M}$ , more than 98.5% of initial fluorescence was quenched, and, at any concentration above that, the quenching effect was the same.  $\text{Ni}^{2+}$  and  $\text{Co}^{2+}$  showed similar titration curves where the fluorescence decrease was rapid at low concentrations and held almost the same residual fluorescence at higher concentrations. However, the quenching effect was weaker compared to  $\text{Cu}^{2+}$ ,  $\text{Ni}^{2+}$  could only quench 61% of the fluorescence and  $\text{Co}^{2+}$  was even less, with 35% as the maximum.  $\text{Fe}^{2+}$  and  $\text{Fe}^{3+}$  showed different titration curve shapes, where the fluorescence change was very small at lower concentration and then dramatically changed with a large margin of error in a small concentration range. After reaching saturation, the fluorescence partially recovered when more cations were added. This suggested a different mechanism of binding and quenching event compared to  $\text{Cu}^{2+}$ ,  $\text{Ni}^{2+}$  and  $\text{Co}^{2+}$ . Further investigation is needed to explore the binding with  $\text{Fe}^{2+}$  and  $\text{Fe}^{3+}$  and the difference between them; however, this paper will focus only on the selectivity and sensitivity of  $\text{Cu}^{2+}$ . Considering all the interfering ions, only  $\text{Cu}^{2+}$  will cause fluorescence quenching more than 79%. Tracing on the curve, it was noted that the concentration of  $\text{Cu}^{2+}$  was 1.37  $\mu\text{M}$  (87.4 parts per billion, ppb) when the quenching percentage reaches 79%. This is still much lower than the EPA action level of  $\text{Cu}^{2+}$  in water which is 1.3 ppm, which means that tmeda-PPpETE can be a viable sensor for  $\text{Cu}^{2+}$  screening.

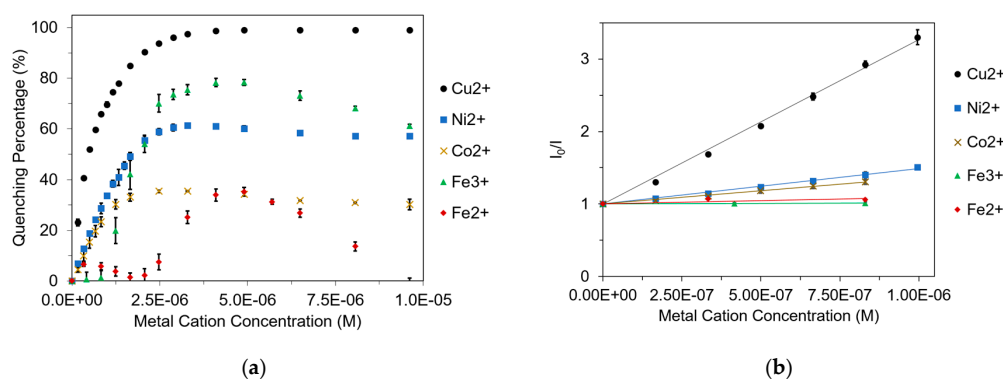


**Figure 6.** (a) fluorescent quenching percentage and (b) Stern–Volmer plot of tmeda-PPpETE upon addition of various concentrations of  $\text{Cu}^{2+}$ ,  $\text{Ni}^{2+}$ ,  $\text{Co}^{2+}$ ,  $\text{Fe}^{2+}$  and  $\text{Fe}^{3+}$ . The quenching percentages were calculated according to the ratio of the remainder fluorescence to the initial fluorescence  $\frac{I_0 - I}{I_0} \times 100\%$ .

To further quantify the quenching efficiency of the tmeda-PPpETE, the fluorescence intensities of the polymer and the concentration of various metal ions were fitted into the Stern–Volmer equation:

$$\frac{I_0}{I} = 1 + K_{SV} [M], \quad (1)$$

where  $I_0$  and  $I$  are the fluorescence intensity of the polymer before and after the addition of metal ions; and  $K_{SV}$  is the Stern–Volmer quenching constant. The results and linear regression are shown in Figure 6b and the values are tabulated in Table 2.

**Table 2.** Summary of linear regression equations,  $R^2$  values and  $K_{SV}$  values for various cations from Stern–Volmer graph.

| Cation Name      | Linear Regression Equation                       | $R^2$ Value | $K_{SV}$           |
|------------------|--|-------------|--------------------|
| Cu <sup>2+</sup> | $\frac{I_0}{I} = 1 + 2.27 \times 10^6 [Cu^{2+}]$ | 1.00        | $2.27 \times 10^6$ |
| Ni <sup>2+</sup> | $\frac{I_0}{I} = 1 + 4.90 \times 10^5 [Ni^{2+}]$ | 1.00        | $4.90 \times 10^5$ |
| Co <sup>2+</sup> | $\frac{I_0}{I} = 1 + 3.63 \times 10^5 [Co^{2+}]$ | 1.00        | $3.63 \times 10^5$ |
| Fe <sup>3+</sup> | $\frac{I_0}{I} = 1 + 1.65 \times 10^4 [Fe^{3+}]$ | 1.00        | $1.65 \times 10^4$ |
| Fe <sup>2+</sup> | $\frac{I_0}{I} = 1 + 9.32 \times 10^4 [Fe^{2+}]$ | 0.39        | $9.32 \times 10^4$ |

The  $K_{SV}$  value of Cu<sup>2+</sup> is an order of magnitude larger than the rest of the ions, indicating good selectivity at low concentrations. The limit of detection (LoD) for Cu<sup>2+</sup> was determined by the following equation:

$$\text{LoD} = \frac{3 \times \sigma}{s}, \quad (2)$$

where  $\sigma$  is the standard deviation of the blank signals; and  $s$  is the slope of the calibration curve. The LoD of Cu<sup>2+</sup> was determined to be  $1.65 \times 10^{-8}$  M or 1.04 ppb ( $\mu\text{g/L}$ ). The high sensitivity of tmeda-PPpETE is capable of screening trace copper under the EPA standard (1.3 ppm).

#### 4. Conclusions

A new FCP, tmeda-PPpETE, with the PPETE conjugated backbone, diamino receptors and pentaipyrene groups was designed and synthesized via the Sonogashira cross coupling reaction. Screening of sixteen common cations showed that this sensor was selective to copper(II) cations with a fluorescent quenching response over 120-fold at  $\lambda_{\text{max}} = 490$  nm. At lower concentrations, the fluorescent quenching and the concentration of Cu<sup>2+</sup> has a linear relationship, with a Stern–Volmer quenching constant  $K_{SV}$  of  $2.27 \times 10^6$ , which is significantly larger than for any other cations. The detection limit of tmeda-PPpETE to Cu<sup>2+</sup> is 1.04 ppb, which is much lower than the EPA action level of 1.3 ppm. This is the first demonstration of the pentaipyrene group participating in metal cation interaction in a polymer system.

**Supplementary Materials:** The following are available online at [www.mdpi.com/2073-4360/9/4/118/s1](http://www.mdpi.com/2073-4360/9/4/118/s1), Synthesis of M1 and butyl-PPpETE, Figure S1: <sup>1</sup>H-NMR of the monomers and the butyl-PPpETE polymer (600 MHz, CDCl<sub>3</sub>); Figure S2: FT-IR of butyl-PPpETE and its corresponding monomers; Figure S3: Emission spectra of the interference studies on the tmeda-PPpETE polymer sensor; Figure S4: Fluorescence emission spectra of tmeda-PPpETE upon addition of different concentrations of Cu<sup>2+</sup>.

**Acknowledgments:** The authors would like to thank Susan Sonner from Corning Inc. (Corning, NY, USA) for the GPC measurements. The research was supported by the Army Research Office (ARO) (W911NF1310235). Research reported in this publication was supported in part by an Institutional Development Award (IDeA) from the National Institute of General Medical Sciences (P20GM103443) and from the National Center for Research Resources (5P20RR016479) of the National Institutes of Health. Additional funding was provided by the Joint Science and Technology Office for Chemical Biological Defense (JSTO-CBD) under contract BA13PHM210. The Bruker Advanced III-600 spectrometer is funded by grant CHE-0922815.

**Author Contributions:** Anting Chen, Megan E. A. Fegley, Sherryllene S. Pinnock and Jetty L. Duffy-Matzner conceived and designed the experiments; Anting Chen and Wei Wu performed the experiments and analyzed the

data with the help from Jetty L. Duffy-Matzner and Wayne E. Jones Jr.; William E. Bernier and Wayne E. Jones Jr. contributed reagents/materials/analysis tools; and Anting Chen wrote most the paper.

**Conflicts of Interest:** The authors declare no conflict of interest.

## References

1. Thomas, S.W.; Joly, G.D.; Swager, T.M. Chemical sensors based on amplifying fluorescent conjugated polymers. *Chem. Rev.* **2007**, *107*, 1339–1386. [[CrossRef](#)] [[PubMed](#)]
2. Fan, L.-J.; Zhang, Y.; Murphy, C.B.; Angell, S.E.; Parker, M.F.L.; Flynn, B.R.; Jones, W.E., Jr. Fluorescent conjugated polymer molecular wire chemosensors for transition metal ion recognition and signaling. *Coord. Chem. Rev.* **2009**, *253*, 410–422. [[CrossRef](#)]
3. Alvarez, A.; Salinas-Castillo, A.; Costa-Fernandez, J.M.; Pereiro, R.; Sanz-Medel, A. Fluorescent conjugated polymers for chemical and biochemical sensing. *TrAC Trends Anal. Chem.* **2011**, *30*, 1513–1525. [[CrossRef](#)]
4. Kim, H.N.; Guo, Z.; Zhu, W.; Yoon, J.; Tian, H. Recent progress on polymer-based fluorescent and colorimetric chemosensors. *Chem. Soc. Rev.* **2011**, *40*, 79–93. [[CrossRef](#)] [[PubMed](#)]
5. Chen, A.; Wu, W.; Jones, W.E., Jr. Polymers and molecular wires as chemical sensors. In *Reference Module in Chemistry, Molecular Sciences and Chemical Engineering*; Elsevier: Cambridge, MA, USA, 2016.
6. Swager, T.M. The molecular wire approach to sensory signal amplification. *Acc. Chem. Res.* **1998**, *31*, 201–207. [[CrossRef](#)]
7. Sakai, R. Conjugated polymers applicable to colorimetric and fluorescent anion detection. *Polym. J.* **2016**, *48*, 59–65. [[CrossRef](#)]
8. Zhou, Q.; Swager, T.M. Fluorescent chemosensors based on energy migration in conjugated polymers: The molecular wire approach to increased sensitivity. *J. Am. Chem. Soc.* **1995**, *117*, 12593–12602. [[CrossRef](#)]
9. Fan, L.J.; Zhang, Y.; Jones, W.E. Design and synthesis of fluorescence “turn-on” chemosensors based on photoinduced electron transfer in conjugated polymers. *Macromolecules* **2005**, *38*, 2844–2849. [[CrossRef](#)]
10. Zhang, Y.; Murphy, C.B.; Jones, W.E. Poly [*p*-(phenyleneethynylene)-*alt*-(thienyleneethynylene)] polymers with oligopyridine pendant groups: Highly sensitive chemosensors for transition metal ions. *Macromolecules* **2002**, *35*, 630–636. [[CrossRef](#)]
11. Jung, H.S.; Kwon, P.S.; Lee, J.W.; Kim, J.I.; Hong, C.S.; Kim, J.W.; Yan, S.; Lee, J.Y.; Lee, J.H.; Joo, T.; et al. Coumarin-derived Cu<sup>2+</sup>-selective fluorescence sensor: Synthesis, mechanisms, and applications in living cells. *J. Am. Chem. Soc.* **2009**, *131*, 2008–2012. [[CrossRef](#)] [[PubMed](#)]
12. Que, E.L.; Domaille, D.W.; Chang, C.J. Metals in neurobiology: Probing their chemistry and biology with molecular imaging. *Chem. Rev.* **2008**, *108*, 1517–1549. [[CrossRef](#)] [[PubMed](#)]
13. Gaggelli, E.; Kozłowski, H.; Valensin, D.; Valensin, G. Copper homeostasis and neurodegenerative disorders (Alzheimer’s, prion, and Parkinson’s diseases and amyotrophic lateral sclerosis). *Chem. Rev.* **2006**, *106*, 1995–2044. [[CrossRef](#)] [[PubMed](#)]
14. Gaetke, L.M.; Chow, C.K. Copper toxicity, oxidative stress, and antioxidant nutrients. *Toxicology* **2003**, *189*, 147–163. [[CrossRef](#)]
15. Tapiero, H.; Townsend, D.M.; Tew, K.D. Trace elements in human physiology and pathology. Copper. *Biomed. Pharmacother.* **2003**, *57*, 386–398. [[CrossRef](#)]
16. Davies, K.M.; Mercer, J.F.B.; Chen, N.; Double, K.L. Copper dyshomeostasis in Parkinson’s disease: Implications for pathogenesis and indications for novel therapeutics. *Clin. Sci.* **2016**, *130*, 565–574. [[CrossRef](#)] [[PubMed](#)]
17. Urucu, O.A.; Aydin, A. Coprecipitation for the determination of copper(ii), zinc(ii), and lead(ii) in seawater by flame atomic absorption spectrometry. *Anal. Lett.* **2015**, *48*, 1767–1776. [[CrossRef](#)]
18. Silberstein, T.; Saphier, M.; Mashiach, Y.; Paz-Tal, O.; Saphier, O. Elements in maternal blood and amniotic fluid determined by ICP-MS. *J. Matern. Fetal Neonatal Med.* **2015**, *28*, 88–92. [[CrossRef](#)] [[PubMed](#)]
19. Attar, T.; Harek, Y.; Larabi, L.L. Determination of copper in whole blood by differential pulse adsorptive stripping voltammetry. *Mediterr. J. Chem.* **2014**, *2*, 691–700.
20. Almeida, E.S.; Richter, E.M.; Munoz, R.A.A. On-site fuel electroanalysis: Determination of lead, copper and mercury in fuel bioethanol by anodic stripping voltammetry using screen-printed gold electrodes. *Anal. Chim. Acta* **2014**, *837*, 38–43. [[CrossRef](#)] [[PubMed](#)]

21. Fan, L.J.; Jones, W.E. Studies of photoinduced electron transfer and energy migration in a conjugated polymer system for fluorescence “turn-on” chemosensor applications. *J. Phys. Chem. B* **2006**, *110*, 7777–7782. [[CrossRef](#)] [[PubMed](#)]
22. Fan, L.-J.; Martin, J.J.; Jones, W.E., Jr. Competition between energy transfer quenching and chelation enhanced fluorescence in a Cu (ii) coordinated conjugated polymer system. *J. Fluoresc.* **2009**, *19*, 555–559. [[CrossRef](#)] [[PubMed](#)]
23. Basabe-Desmonts, L.; Reinhoudt, D.N.; Crego-Calama, M. Design of fluorescent materials for chemical sensing. *Chem. Soc. Rev.* **2007**, *36*, 993–1017. [[CrossRef](#)] [[PubMed](#)]
24. Gu, C.; Huang, N.; Gao, J.; Xu, F.; Xu, Y.H.; Jiang, D.L. Controlled synthesis of conjugated microporous polymer films: Versatile platforms for highly sensitive and label-free chemo- and biosensing. *Angew. Chem. Int. Ed.* **2014**, *53*, 4850–4855. [[CrossRef](#)] [[PubMed](#)]
25. Gu, C.; Huang, N.; Wu, Y.; Xu, H.; Jiang, D. Design of highly photofunctional porous polymer films with controlled thickness and prominent microporosity. *Angew. Chem. Int. Ed.* **2015**, *54*, 11540–11544. [[CrossRef](#)] [[PubMed](#)]
26. Pinnock, S.S.; Malele, C.N.; Che, J.; Jones, W.E., Jr. The role of intermolecular interactions in solid state fluorescent conjugated polymer chemosensors. *J. Fluoresc.* **2012**, *22*, 583–589. [[CrossRef](#)] [[PubMed](#)]
27. Nie, H.R.; Sun, G.N.; Zhang, M.; Baumgarten, M.; Mullen, K. Fluorescent conjugated polycarbazoles for explosives detection: Side chain effects on tnt sensor sensitivity. *J. Mater. Chem.* **2012**, *22*, 2129–2132. [[CrossRef](#)]
28. Zhang, G.W.; Lu, X.M.; Wang, Y.Y.; Huang, Y.Q.; Fan, Q.L.; Huang, W. Water-soluble fluorescent nanoparticles without distinct aggregation of conjugated polymer chains. *Polym. Int.* **2011**, *60*, 45–50. [[CrossRef](#)]
29. Yang, J.-S.; Swager, T.M. Porous shape persistent fluorescent polymer films: An approach to tnt sensory materials. *J. Am. Chem. Soc.* **1998**, *120*, 5321–5322. [[CrossRef](#)]
30. Yang, J.-S.; Lin, C.-S.; Hwang, C.-Y. Cu<sup>2+</sup>-induced blue shift of the pyrene excimer emission: A new signal transduction mode of pyrene probes. *Org. Lett.* **2001**, *3*, 889–892. [[CrossRef](#)] [[PubMed](#)]
31. Cao, J.; Guo, J.B.; Li, P.F.; Chen, C.F. Complexation between pentaerythritol derived bis(crown ether)s and CBPQT(4+) salt: Ion-controlled switchable processes and changeable role of the CBPQT(4+) in host-guest systems. *J. Org. Chem.* **2011**, *76*, 1644–1652. [[CrossRef](#)] [[PubMed](#)]
32. Barton, T. Processible poly [(p-phenyleneethynylene)-alt-(2, 5-thienyleneethynylene)]s of high luminescence: Their synthesis and physical properties. *J. Mater. Chem.* **1998**, *8*, 1687–1690.
33. Mandal, S. Studies in sulfur heterocycles. Part 15. Condensed heterocycles derived from thieno [2, 3-c]- and thieno [3, 2-c]-thiopyrans. *J. Chem. Soc. Perkin Trans. 1* **1999**, 2639–2644. [[CrossRef](#)]
34. Zhu, X.-Z.; Chen, C.-F. Iptycene quinones: Synthesis and structure. *J. Org. Chem.* **2005**, *70*, 917–924. [[CrossRef](#)] [[PubMed](#)]
35. Yang, J.-S.; Swager, T.M. Fluorescent porous polymer films as tnt chemosensors: Electronic and structural effects. *J. Am. Chem. Soc.* **1998**, *120*, 11864–11873. [[CrossRef](#)]
36. Bunz, U.H. Poly (aryleneethynylene)s: Syntheses, properties, structures, and applications. *Chem. Rev.* **2000**, *100*, 1605–1644. [[CrossRef](#)] [[PubMed](#)]
37. Mallory, F.B.; Baker, M.B. Studies of magnetic anisotropy. 2. NMR evidence for the existence of deshielding regions alongside carbon-carbon triple bonds. *J. Org. Chem.* **1984**, *49*, 1323–1326. [[CrossRef](#)]
38. Yang, J.S.; Yan, J.L. Central-ring functionalization and application of the rigid, aromatic, and H-shaped pentaerythritol scaffold. *Chem. Commun.* **2008**, 1501–1512. [[CrossRef](#)] [[PubMed](#)]
39. Wang, Z.H.; Wang, Z.Y.; Ma, J.J.; Bock, W.J.; Ma, D.G. Effect of film thickness, blending and undercoating on optical detection of nitroaromatics using fluorescent polymer films. *Polymer* **2010**, *51*, 842–847. [[CrossRef](#)]
40. Ghosh, K.R.; Saha, S.K.; Wang, Z.Y. Ultra-sensitive detection of explosives in solution and film as well as the development of thicker film effectiveness by tetraphenylethene moiety in active fluorescent conjugated polymer. *Polym. Chem.* **2014**, *5*, 5638–5643. [[CrossRef](#)]
41. Enlow, M.A. Binding of tnt to amplifying fluorescent polymers: An ab initio and molecular dynamics study. *J. Mol. Graph. Model.* **2012**, *33*, 12–18. [[CrossRef](#)] [[PubMed](#)]
42. Fegley, M.E.A.; Pinnock, S.S.; Malele, C.N.; Jones, W.E., Jr. Metal-containing conjugated polymers as fluorescent chemosensors in the detection of toxicants. *Inorg. Chim. Acta* **2012**, *381*, 78–84. [[CrossRef](#)] [[PubMed](#)]

43. Liu, Y.; Wu, P.; Jiang, J.; Wu, J.; Chen, Y.; Tan, Y.; Tan, C.; Jiang, Y. Conjugated polyelectrolyte nanoparticles for apoptotic cell imaging. *ACS Appl. Mater. Interfaces* **2016**, *8*, 21984–21989. [[CrossRef](#)] [[PubMed](#)]
44. Xu, H.; Wu, W.; Chen, Y.; Qiu, T.; Fan, L.-J. Construction of response patterns for metal cations by using a fluorescent conjugated polymer sensor array from parallel combinatorial synthesis. *ACS Appl. Mater. Interfaces* **2014**, *6*, 5041–5049. [[CrossRef](#)] [[PubMed](#)]
45. Fegley, M.E.; Sandgren, T.; Duffy-Matzner, J.L.; Chen, A.; Jones, W.E. Detection and differentiation of ferrous and ferric ions using fluorescent metallopolymer and oligomer chemosensors. *J. Polym. Sci. Part A Polym. Chem.* **2015**, *53*, 951–954. [[CrossRef](#)]
46. Fan, L.-J.; Jones, W.E. A highly selective and sensitive inorganic/organic hybrid polymer fluorescence “turn-on” chemosensory system for iron cations. *J. Am. Chem. Soc.* **2006**, *128*, 6784–6785. [[CrossRef](#)] [[PubMed](#)]



© 2017 by the authors. Licensee MDPI, Basel, Switzerland. This article is an open access article distributed under the terms and conditions of the Creative Commons Attribution (CC BY) license (<http://creativecommons.org/licenses/by/4.0/>).